

# Spacecraft Design Fundamentals Report

Group 7

**Jessica Hauschulz**

**Jose Roberto Aguiñaga Ortiz**

**Alesander Oteo**

**Kiyan Boetzel**

**Keval Ghetiya**

Thesis for the attainment of the academic degree

**Master of Science (M.Sc.) Aerospace**

at the TUM School of Engineering and Design of the Technical University of Munich.

**Examiner:**

Prof. Alessandro Golkar

**Supervisor:**

Vincenzo Messina

**Submitted:**

Munich, 21.07.2024

# Contents

<b>1</b>	<b>Introduction (written by Roberto, designed all)</b>	<b>1</b>
1.1	Mission Objectives . . . . .	1
1.1.1	Primary Objective . . . . .	1
1.1.2	Secondary Objective . . . . .	1
<b>2</b>	<b>Main Requirements (written by all)</b>	<b>2</b>
<b>3</b>	<b>Subsystem Requirements (designed by each subsystem team)</b>	<b>3</b>
<b>4</b>	<b>System Architecture</b>	<b>5</b>
4.1	System . . . . .	5
4.1.1	Mass and Power Budgets (all) . . . . .	5
4.1.2	Link Budget (Alesander Oteo) . . . . .	5
4.2	Mission Orbit & DeltaV (Keval Ghetiya and Kiyan Boetzel) . . . . .	5
4.2.1	Orbital Parameters of the Target Orbit . . . . .	5
4.2.2	Sun Light and Eclipse Time . . . . .	6
4.2.3	Deorbit Maneuver . . . . .	6
4.3	Propulsion System (Jessica Hauschulz, Keval Ghetiya) . . . . .	7
4.3.1	Brief Trade-off of Different Propulsion Systems . . . . .	7
4.3.2	Type of Propulsion System Selected with Main Parameters . . . . .	8
4.4	Launcher Selection (Keval Ghetiya, Kiyan Boetze) . . . . .	9
4.5	Spacecraft . . . . .	10
4.5.1	Payload (Roberto Aguiñaga and Kiyan Boetzel) . . . . .	10
4.5.2	Attitude Determination and Control System (ADCS) (Keval Ghetiya) . . . . .	14
4.5.3	Power (Alesander Oteo, Jessica Hauschulz) . . . . .	16
4.5.4	TT&C (Alesander Oteo) . . . . .	18
4.5.5	Ground Segment (Alesander Oteo) . . . . .	21
4.5.6	Structure (Roberto Aguiñaga and Kiyan Boetzel) . . . . .	22
4.5.7	Thermal (Roberto Aguiñaga, Jessica Hauschulz) . . . . .	23
4.6	Conclusion (Roberto Aguiñaga) . . . . .	25
<b>Bibliography</b>		<b>26</b>

# List of Figures

4.1	Inclination $i$ , RAAN $\Omega$ , and Sun-Angle $\beta$ plotted over the 5 year mission duration . . . . .	6
4.2	Schematic of Propulsion System . . . . .	9
4.3	Sony & Prophesee visual representation of results with Event Filtering (left) and without it [4] . . . . .	11
4.4	Graphic representation of bandwidth reduction capabilities for Event-based Sensors by Samsung [2] . . . . .	11
4.5	Cassegrain Telescope Layout . . . . .	12
4.6	Secondary Lens Diameter and Sensor Distance depending on primary Focal Length . . . . .	13
4.7	ADSC System [23] . . . . .	16
4.8	DoD for a Lithium Ion Battery . . . . .	18
4.9	TLE format structure [1] . . . . .	19
4.10	Typical TT&C structure . . . . .	20
4.11	Vehicle Dimensions, Structure, and Modules (Stowed) . . . . .	22
4.12	Final deployed Configuration . . . . .	23
4.13	Reference Satellite CAS 500 from Korean Aerospace Research Institute [6] . . . . .	24

# List of Tables

1.1 Primary Mission Objectives . . . . .	1
1.2 Secondary Mission Objectives . . . . .	1
2.1 Main Requirements . . . . .	2
3.1 Orbit Subsystem Requirements . . . . .	3
3.2 Payload Subsystem Requirements . . . . .	3
3.3 Attitude Determination and Control System (ADCS) Requirements . . . . .	3
3.4 Thermal Subsystem Requirements . . . . .	4
3.5 Propulsion Subsystem Requirements . . . . .	4
3.6 Power Subsystem Requirements . . . . .	4
3.7 Communication Subsystem Requirements . . . . .	4
4.1 Component Mass distribution . . . . .	5
4.2 Power consumption . . . . .	5
4.3 Link Budget . . . . .	5
4.4 Orbital Parameters . . . . .	6
4.5 Pugh Matrix for Propulsion Systems with Weighted Scores . . . . .	7
4.6 Delta-v Requirements . . . . .	8
4.7 Thruster Characteristics . . . . .	8
4.8 Comparison of Propulsion Systems . . . . .	9
4.9 Detailed Parameters of Monopropellant System . . . . .	9
4.10 Event-based sensor specifications [13] [11] [3] . . . . .	10
4.11 Final optical system specifications . . . . .	13
4.12 Processor and data recorder specifications. [7] . . . . .	13
4.13 Power Consumers and Their Operating Periods . . . . .	16
4.14 Power Subsystem Results . . . . .	19
4.15 Structure of the Message . . . . .	19
4.16 Values used and results of the TTC subsystem . . . . .	21
4.17 Selected Ground Stations . . . . .	21
4.18 Component Mass distribution . . . . .	23

# 1 Introduction (written by Roberto, designed all)

Space debris is a growing problem in space exploration, which already has generated contained incidents in satellite impacts, visual interferences in astronomical observation, and has an increasing potential of making space missions impossible. Collisions between different debris represents an exponential increase of this problem, to have collision detection capabilities in spacecraft will become critical to generate data for debris increase tendencies and integrate autonomous navigation as well as evasive maneuvers. The European Union currently relies in foreign space debris catalogs, to enhance the regulations of space debris and end-of-life operations, there is a requirement for a separate European database. It would be beneficial to gather data for this catalogue. For access to detailed calculations, it is possible to consult them in the following github repository: [https://github.com/Alesander-oteo/spacecraft\\_calcs.git](https://github.com/Alesander-oteo/spacecraft_calcs.git).

## 1.1 Mission Objectives

The mission is designed with the aim of detecting transient debris, as well as tracking tendencies in a monitored debris conjunction in SSO by applying Event Camera technologies with Artificial Intelligence enhancements. Data gathering shall be used as well to generate a European Union specific Space debris catalogue. [22]

### 1.1.1 Primary Objective

Evaluate Event camera capabilities for collision detection in monitored space conjunctions.

**Table 1.1** Primary Mission Objectives

ID	Objectives
PO1	Evaluate Event camera capabilities for collision detection in monitored space conjunctions.

### 1.1.2 Secondary Objective

Identify and categorize “visible” debris conjunctions in SSO. By providing real-time data on space debris movements, this mission can enhance space situational awareness (SSA) and help prevent collisions.

**Table 1.2** Secondary Mission Objectives

ID	Objectives
SO1	Identify and categorize “visible” debris conjunctions in SSO.
SO2	By providing real-time data on space debris movements, this mission can enhance space situational awareness (SSA) and help prevent collisions.

## 2 Main Requirements (written by all)

**Table 2.1** Main Requirements

ID	Requirement	Source
MR1	The spacecraft shall be launched in 2027.	PO1
MR2	The spacecraft shall have mass (weight) ranging from 100 to 500 kg.	PO1
MR3	The spacecraft shall comply with the international regulations for end-of-life disposal.	PO1
MR4	The spacecraft shall remain operational for 5 years.	PO1
MR5	The spacecraft shall record for 8 minutes at the north pole conjunctions.	SO2
MR6	The data gathered shall be transmitted to ground operations for image reconstruction.	SO2
MR7	The spacecraft shall scan debris conjunctions in SSO between 6 and 10 cm.	SO1, SO2
MR8	The spacecraft shall maintain a Sun Synchronous Orbit.	SO1
MR9	The spacecraft shall process imagery into data for categorization.	SO1
MR10	The spacecraft shall maintain the attitude to ensure the defined area monitoring.	SO1
MR11	The spacecraft shall have a fail-safe mode for communications.	PO1
MR12	The spacecraft shall be launched in Falcon 9 from Launch Site: Vandenberg AFB Space Launch Complex 4.	PO1
MR13	The launcher shall put the spacecraft in the target orbit.	PO1
MR14	The spacecraft shall withstand vibrations during the launch without structure failure.	PO1
MR15	The system shall operate with one single spacecraft.	PO1
MR16	The spacecraft shall be capable of being powered throughout the entire mission.	PO1
MR17	The spacecraft shall be capable of powering all consumers simultaneously.	PO1
MR18	The spacecraft shall have the capacity to operate during eclipse periods.	PO1
MR19	The spacecraft shall have power redundancy in case of component failure.	PO1

## 3 Subsystem Requirements (designed by each subsystem team)

**Table 3.1** Orbit Subsystem Requirements

ID	Requirement	Source
OR1	The spacecraft shall have an orbital period of 6000s.	PO1
OR2	The spacecraft shall have a maximum of 20% of eclipse time per orbit.	PO1
OR3	The spacecraft shall maintain a Sun Synchronous Orbit.	PO1

**Table 3.2** Payload Subsystem Requirements

ID	Requirement	Source
PL1	Event Camera shall have a resolution of 6 cm.	PO1
PL2	Event Camera shall have a power consumption of 5 W for the sensor.	PO1
PL3	Event Camera shall have a data rate of 1.6 Gbits per second.	PO1
PL4	Event Camera shall have wavelength sensitivity of 400 to 700 nm.	PO1
PL5	Event Camera shall be able to detect objects of 6 to 10 cm.	PO1
PL6	The entire optics system shall not surpass a length of 1.5 m.	PO1
PL7	Payload shall be able to store recorded data in case of emergencies.	SO1
PL8	Payload shall process and compress the recorded data.	SO1

**Table 3.3** Attitude Determination and Control System (ADCS) Requirements

ID	Requirement	Source
AD1	The subsystem shall provide a pointing accuracy of 1 degree.	PO1
AD2	The subsystem shall be able to slew the spacecraft at a rotational rate of 0.1 degrees per second.	PO1
AD3	The subsystem shall use a 3-axis stability technique to reject external (and internal) disturbance torques.	PO1
AD4	The subsystem shall include three reaction wheels as the main actuators for the three axes, with one additional reaction wheel for redundancy.	PO1
AD5	The subsystem shall incorporate cold-gas thrusters as secondary actuators to dump the momentum created by the reaction wheels when necessary, and for small correction maneuvers.	PO1
AD6	The subsystem shall have 6 sun-sensors, 2 horizon sensors, and a magnetometer to determine the attitude of the spacecraft.	PO1
AD7	Each reaction wheel shall have 10 mNm of torque and 0.5 Nms of momentum storage capacity.	PO1
AD8	Each cold-gas thruster shall be able to produce 0.25 N of thrust.	PO1

**Table 3.4** Thermal Subsystem Requirements

ID	Requirement	Source
TH1	System shall ensure a minimal operational temperature of 0° Celsius for cold cases.	PO1
TH2	System shall ensure a maximal operational temperature of 30° Celsius for hot cases.	PO1
TH3	System shall actively heat critical components if a 0° Celsius temperature is not passively ensured.	PO1

**Table 3.5** Propulsion Subsystem Requirements

ID	Requirement	Source
PR1	The spacecraft shall have a propulsion system containing 4 monopropellant thrusters and 6 cold-gas thrusters.	PO1
PR2	The spacecraft shall have two propellant tanks, one containing Nitrogen pressurant gas, and the other containing Hydrazine as monopropellant.	PO1
PR3	The pressurant tank shall be able to store Nitrogen at 200 bar and 15°C temperature.	PO1
PR4	The propellant tank shall be able to store Hydrazine at 23 bar and 23°C temperature.	PO1
PR5	The spacecraft shall use monopropellant thrusters as the main propulsion unit, providing 100 N total thrust, during maintenance manoeuvres and de-orbiting maneuver.	PO1

**Table 3.6** Power Subsystem Requirements

ID	Requirement	Source
PW1	The spacecraft shall be able to generate "295" W from solar panels.	PO1
PW2	The spacecraft shall have an onboard battery of "205" Wh.	PO1
PW3	The spacecraft shall have an onboard solar array of "1.5" m <sup>2</sup>	PO1
PW4	The system shall power the spacecraft after 5 years	PO1

**Table 3.7** Communication Subsystem Requirements

ID	Requirement	Source
CM1	The system shall transmit the processed data to the ground station with a latency of less than "tbd" hours.	SO2
CM2	The system shall provide global coverage to communicate with the satellite	SO2
CM3	The system shall transmit the required data in an organized manner	SO2

# 4 System Architecture

## 4.1 System

### 4.1.1 Mass and Power Budgets (all)

Component	Mass [kg]	Mass Fraction [%]
Payload	27.92	11.99
Power	14.01	6.02
TT&C	9.75	4.19
Thermal	0.02	0.009
Propulsion	87.04	34.39
ADCS	34.08	14.64
Structure	60.01	25.78
<b>Total <math>m_{B.o.L.}</math></b>	<b>232.79</b>	

Table 4.1 Component Mass distribution

Component	Power [W]	Power Fraction [W]
Payload	100.5	35%
Power	10	3%
TT&C	25	8%
Thermal	80	27%
Propulsion	66	22%
ADCS	13.75	5%
Structure	0	0%
<b>Total W</b>	<b>295.25</b>	

Table 4.2 Power consumption

### 4.1.2 Link Budget (Alesander Oteo)

Parameter	Value
Antenna Power (dBm)	36.02
Antenna Gain (dB)	7
Frequency Satellite (Hz)	$2.1 \times 10^9$
Frequency Ground (Hz)	$2.03 \times 10^9$
Receiving Antenna Gain (dB)	40
EIRP (dBm)	42.91
Free Space Path Loss (FSPL) (dB)	118.33

Table 4.3 Link Budget

## 4.2 Mission Orbit & DeltaV (Keval Ghetiya and Kiyan Boetzel)

A mixture of analytical parameter calculation and numerical calculation through the software tool *GMAT* yielded the parameters shown below.

### 4.2.1 Orbital Parameters of the Target Orbit

A sun synchronous orbit exploits the J2-perturbation to advance the RAAN (Right Angle Ascension of Nodes) by a rate of  $1.7202 \times 10^{-2} \text{ d}^{-1}$ , yielding a total RAAN change and related rotation of the orbital plane by  $360^\circ$  per year. According to [21], orbit inclination, major semi-axis and eccentricity are related by the following expression:

$$\cos i = -0.098917 \cdot (1 - e^2)^2 \left( \frac{a}{r_{Earth}} \right)^{\frac{7}{2}} \quad (4.1)$$

Where  $e$  is the orbit eccentricity,  $a$  the semi-major-axis,  $r_{Earth}$  the radius of the earth, and  $i$  the inclination. For a quasi-circular orbit ( $e \approx 0$ ) the semi-major-axis calculation reduces to:

$$a = r_{Earth} \cdot \left( \frac{\cos i}{-0.098917} \right)^{\frac{2}{7}} \quad (4.2)$$

A chosen inclination of  $i = 98.6^\circ$  yields a semi-major-axis (here also radius) of  $a = 7177.32$  km. The final orbital parameters are shown in Table 4.4, as well as in Fig.4.1 as a function of time.

Parameter	Symbol	Value
Inclination	$i$	$98.6^\circ$
Semi-Major-Axis / Radius	$a$	7177.32 km
Altitude	$H_{Orbit}$	799.32 km
Eccentricity	$e$	$\approx 0$
Orbital Period	$t$	6051.39 s
Max. Eclipse Time	$T_{Eclipse,max}$	1107.8 s
Sun Angle	$\beta$	$57.6^\circ - 89.8^\circ$
RAAN-Change-Rate	$\frac{\partial \Omega}{\partial t}$	$1.7202 \times 10^{-2} \text{ d}^{-1}$

**Table 4.4** Orbital Parameters

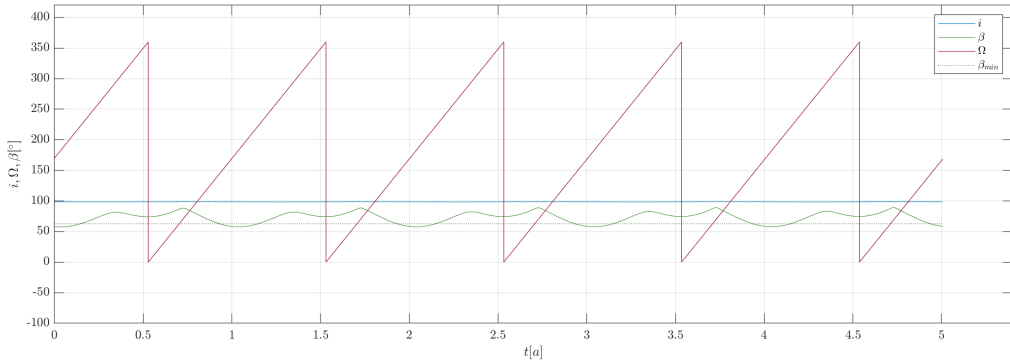


**Figure 4.1** Inclination  $i$ , RAAN  $\Omega$ , and Sun-Angle  $\beta$  plotted over the 5 year mission duration

## 4.2.2 Sun Light and Eclipse Time

The sun angle  $\beta$  was calculated through a *GMAT* script, yielding a high variability between  $57.6^\circ$  and  $89.8^\circ$ . The orbit is non-ecliptic if:

$$\beta > \arcsin \frac{r_{earth}}{a} \quad (4.3)$$

which for the chosen orbit yields a minimum sun angle  $\beta_{min} = 62.7^\circ$ . It follows that the space craft will experience some eclipse time over the course of the year. The minimum sun angle  $\beta_{min}$  is included in Fig.4.1, showing the periods where the orbit is ecliptic. These ecliptic periods are occurring over the south pole, while the north pole, the area of observation, remain non-ecliptic throughout the mission duration. The maximum eclipse time was given by *GMAT* as  $T_{Eclipse,max} = 1107.8$  s, as seen in Tab.4.4.

## 4.2.3 Deorbit Maneuver

The DeltaV required to deorbit the vehicle was calculated based on [23]:

$$\Delta V_{Deorbit} = V_{Orbit} \frac{1 - \sqrt{2(r_{Earth} + H_{Perigee})}}{2r_{Earth} + H_{Perigee} + H_{Orbit}} \quad (4.4)$$

With orbital velocity  $V_{Orbit} = 7452.3 \text{ m s}^{-1}$ , an initial altitude  $H_{Orbit} = 799.32 \text{ km}$ , and a chosen perigee altitude  $H_{Perigee} = 300.00 \text{ km}$  ( $r_{Earth} = 6378.00 \text{ km}$ ) this yields:  $\Delta V_{Deorbit} = 135.72 \text{ m s}^{-1}$ .

## 4.3 Propulsion System (Jessica Hauschulz, Keval Ghetiya)

The purpose of the onboard propulsion system of the spacecraft is to provide the thrust needed for maintenance manoeuvres during the lifetime and de-orbiting manoeuvres at the end of the life. It is assumed that the launcher will put the spacecraft into the target orbit. The propulsion system was developed based on a trade-off study, a further comparison of three systems by calculations and a detailed design of the chosen mono-propellant system.

### 4.3.1 Brief Trade-off of Different Propulsion Systems

To compare various propulsion systems for the spacecraft, a Pugh matrix, see table 4.5, was created to evaluate each system based on a set of criteria. Each criterion was assigned a weight to reflect its importance, and each propulsion system was rated from 1 to 3. The total score for each system was calculated by summing the weighted scores for all criteria. 1 represents the least favorable performance and 3 the most favorable one. The following table presents the Pugh matrix with weighted scores:

**Table 4.5** Pugh Matrix for Propulsion Systems with Weighted Scores

Criteria	Weight	Mono-propellant	Bi-propellant	Cold Gas	Hall Effect	Ion Thrusters	Solar Sail	Nuclear
Specific Impulse (Isp)	3	1	2	1	3	3	2	2
Thrust-to-Weight Ratio	2	2	2	1	1	1	1	3
Efficiency	2	2	3	2	3	3	2	2
Cost	1	2	1	2	1	1	3	1
Reliability	2	3	3	3	1	2	2	1
Maturity of Technology	1	3	2	3	2	2	2	1
Complexity	2	3	2	3	1	1	1	1
Size and Mass	1	2	1	2	2	1	3	1
Scalability	2	3	2	2	3	3	2	2
Fuel Availability	1	3	2	3	3	2	3	1
<b>Total Score</b>		<b>50</b>	<b>38</b>	<b>40</b>	<b>39</b>	<b>46</b>	<b>39</b>	<b>30</b>

Based on these criteria, we've identified cold gas thrusters, mono-propellant chemical propulsion, and electric ion thrusters as most interesting for further exploration.

#### Cold Gas Thrusters:

Cold gas thrusters are favored for their simplicity, reliability, and cost-effectiveness. They are easy to operate and ideal for short-term maneuvers and precise attitude control, though they have lower efficiency for long-duration missions due to their lower specific impulse.

#### Monopropellant Chemical Propulsion:

Monopropellant thrusters offer a balance of cost, reliability, and simplicity. They are efficient for short maneuvers with a good thrust-to-weight ratio, making them suitable for missions requiring quick, responsive thrust. Their well-established technology ensures dependable performance.

#### Electric Ion Thrusters:

Electric ion thrusters provide exceptionally high specific impulse, making them the best choice for long-duration missions. Despite their complexity and higher initial costs, their superior fuel efficiency and ability to perform precise trajectory adjustments make them valuable for extended missions.

Further investigation into these systems will optimize the propulsion strategy, ensuring a successful and efficient mission.

### 4.3.2 Type of Propulsion System Selected with Main Parameters

Furthermore, a detailed analysis of the propulsion system and delta-v requirements for a spacecraft was conducted using a MATLAB script. The script calculates the delta-v needed for orbit maintenance and de-orbiting, evaluates the propellant masses for different propulsion systems, and determines the total system masses. The performance of the different propulsion systems are compared and a the lightest and simplest propulsion for our system is chosen. All calculations are based on The new SMAD [23]

#### Delta-v Requirements

Delta-v calculations follow the SMAD process. The delta-v needed for orbit maintenance accounts for drag and solar radiation pressure (SRP). The total delta-v combines these maintenance needs with the delta-v required for de-orbiting, see equation 4.4, calculated from orbital velocity and altitude changes. The outputs are shown in table 4.6.

Delta-v Requirements	Value
Total delta-v for orbit maintenance over 5 years	225.46 m/s
Delta-v for deorbiting	135.72 m/s
Total Delta-v required	361.18 m/s

Table 4.6 Delta-v Requirements

#### Propellant and Pressurant Calculations

Table 4.7 summarizes different thruster types. The mass of propellant is derived from the Tsiolkovsky rocket equation, relating delta-v to specific impulse (Isp) and gravitational acceleration.

Thruster Type	Specific Impulse (s)	Efficiency	Propellant
Ion thruster	3000	0.7	Xenon
Cold gas thruster	60	0.5	Nitrogen
Monopropellant thruster	250	0.55	Hydrazine
Pressurant for monopropellant	-	-	Nitrogen

Table 4.7 Thruster Characteristics

Using Professor Chiara Manfleittis's lecture notes [9], tank dimensions for propellant and pressurant are calculated to ensure they withstand operational pressures. The tanks are sized as spherical aluminium tanks for simplicity reasons. The tank masses are calculated based on their dimensions and material densities, with the total tank mass including both propellant and pressurant tanks, see table 4.9.

#### Comparison of Propellant and System Mass

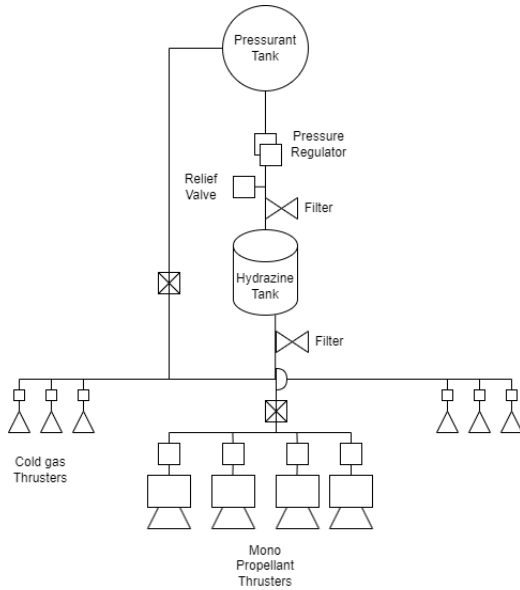
Table 4.8 compares the propellant mass and total system mass for the three thruster types. For further calculations a 10 percent margin is added ontop of the propellant, and pressurant, system to avoid running out of propellant before the end of lifetime.

#### Choice of Monopropellant System

Propulsion System	Propellant Mass (kg)	Total System Mass (kg)
Monopropellant Thruster	41.09	49.58
Ion Thruster	3.66	13.66
Cold Gas Thruster	137.62	142.62

**Table 4.8** Comparison of Propulsion Systems

The monopropellant system was selected for its lower total mass, which reduces launch costs and simplifies integration. Despite having a lower specific impulse and higher mass than the ion thruster, it meets mission needs effectively with a simpler, cost-effective design. The basic schematic of the chosen propulsion system is given in 4.2 as well as the characteristics in 4.9.

**Figure 4.2** Schematic of Propulsion System

The system is equipped with four mono-propellant thrusters (MR-106L) [12], strategically positioned to provide the necessary thrust for precise maneuvering and attitude control. This configuration not only delivers the required thrust for mission operations but also incorporates redundancy to enhance system reliability. Additionally, 6 cold gas thrusters utilizing the pressurant Nitrogen are added for ADCS.

Parameter	Propellant	Pressurant
Mass (kg)	41.09	0.04
Volume ( $m^3$ )	0.0443	0.0213
Radius (m)	0.2195	0.1719
Wall Thickness (m)	0.0015	0.0023
Total Tank Mass (kg)	2.47	2.38
Total Propulsion System Mass	48 kg	

**Table 4.9** Detailed Parameters of Monopropellant System

#### 4.4 Launcher Selection (Keval Ghetiya, Kiyan Boetze)

The Falcon 9 [16] by SpaceX was chosen for its proven reliability, cost-effectiveness, and versatility. Its strong track record and reusability reduce launch costs while maintaining high performance. Falcon 9's capability to deliver payloads to LEO SSO target orbit makes it ideal for this missions. SpaceX offers

Rideshare Missions [15], [14] for small spacecraft on the Falcon 9 Launch Vehicle and that is selected for this mission by considering the spacecraft structure.

The launch site is Vandenberg AFB Space Launch Complex 4 (SLC-4), optimal for polar and sun-synchronous orbits. Vandenberg's west coast location, state-of-the-art facilities, robust logistical support, and established safety protocols ensure a smooth, reliable launch process.

## 4.5 Spacecraft

### 4.5.1 Payload (Roberto Aguiñaga and Kiyan Boetzel)

#### Optics

The first approach considered for the sizing of the optics was to perform the same process that was used during the exercise. Considering the rate limitation of 500 kilometers of altitude to 1 meter of ground sampling distance, Roberto applied a 1-meter focal length and a 700-nanometer wavelength as the first iteration to evaluate how the diameter and pixel radius dimensions would behave.

$$D = \frac{2.44 \cdot \lambda \cdot h \cdot GSD}{f} = 0.85 \text{ m} \quad (4.5)$$

$$r_{\text{pixel}} = \frac{GSD \cdot f}{h} = 2 \mu\text{m} \quad (4.6)$$

With the obtained diameter of 85 cm and a pixel radius of 2 micrometers, a benchmark study was conducted to evaluate event-based sensors available in the market and their real capabilities. The research done was also considering the specifications required for the sizing of power, thermal, and telecommunications systems. The main event-based sensor manufacturers can be observed in the following table.

Specification	Samsung DVS Gen 4	Prophesee EVK 4	Sony IMX6
Array size	1280x960	1280x720	1280x720, 640x512
Pixel Radius	4.95 $\mu\text{m}$	4.86 $\mu\text{m}$	4.86 $\mu\text{m}$
Data Rate	1 Gb/s	1.6 Gb/s	1.56 Gb/s
Power Consumption	5 W	750 mW	750 mW
Mass	Not Available	95 g (Module)	Not Available
Compression	Coincidence Detection	Event Filter	Event Filter
Price	Not Available	4000 EUR	Not Available

Table 4.10 Event-based sensor specifications [13] [11] [3]

As can be observed, all the event-based specific sensors are standardized for a pixel size of 4 to 5 micrometers, hence having a 2 micrometers specification for the payload pixel was not a feasible option. Addressing this question with the tutors, it was verified that taking the market as a baseline was a correct approach for payload sizing given the ground sampling distance limitation. Regarding the rest of the specifications, Sony's and Prophesee catalogue are similar in all aspects since their sensors are a collaborative work between both companies, while Samsung's offer represented greater pixel radius and power consumptions. Finally, the decision came to the greatest amount of information available about the product to be able to size the rest of the components more accurately. The selected sensor was the Prophesee EVK4 module.

Needed for the telecommunications system, the data rate was a relevant specification to consider. The EVK4 system official datasheet states a maximum data output of 1.6 Gb per second, the same value that is stated as the limit for this space mission by the project requirements. It is important to mention

that this is a maximum output when all the pixels are being activated by a potential event, and that this value can be reduced by the anti-flicker event filter and event rate control capabilities that the module offers. Hence, the system selected for the mission payload will be able to regulate the data output that the telecommunications system shall send to ground stations.

As a verification of the availability of these technologies, the Samsung event-based sensors also serve as a suitable example for this. Their development team has also worked on algorithms for event-stream compression to detect coincidences in the detected events by the pixels, which in some cases lead to the 99.6 percent reduction of the bandwidth. These filtering features are commonly offered in the market due to the automation applications of event-based cameras where low bandwidths are needed.

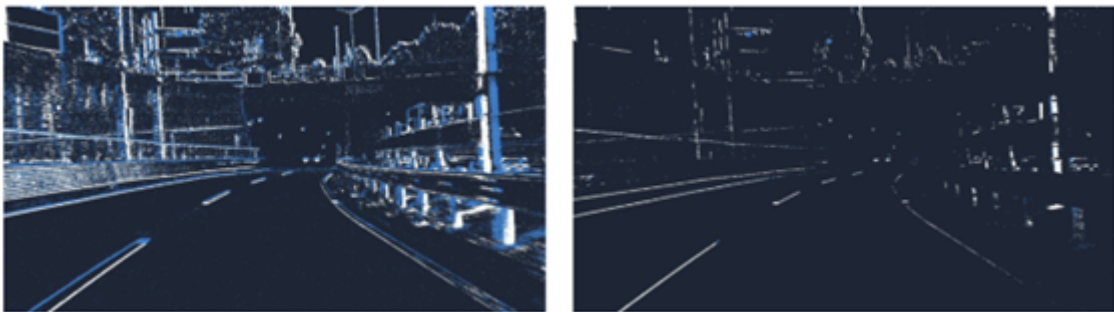


**Figure 4.3** Sony & Prophesee visual representation of results with Event Filtering (left) and without it [4]

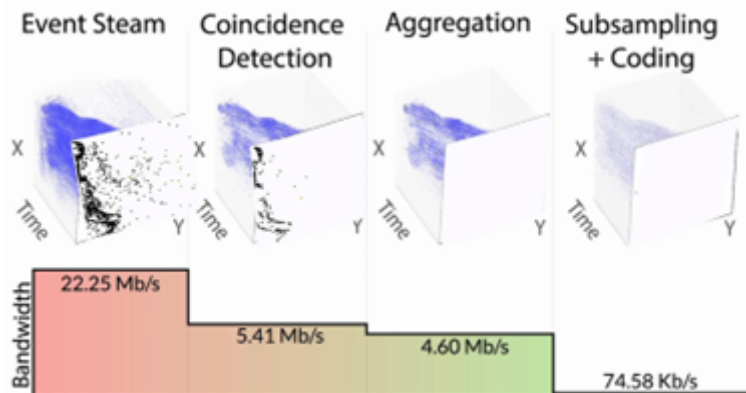


**Figure 4.4** Graphic representation of bandwidth reduction capabilities for Event-based Sensors by Samsung [2]

With the pixel specifications fixed and the defined distance to the objective orbit of 40 kilometers, a MATLAB code was set up to mainly obtain the focal length and diameter of the optical system. At this point is where the team encountered the consequence of the GSD rate stated for the project. The resultant focal length was 2.4 meters and the diameter was 35 centimeters. While the diameter represents no significant tradeoff for the overall spacecraft structure sizing, a 2.4-meter optical system in length represents significant increases in mass, dimensions, and power for the spacecraft. The MATLAB code "ARRAYFINAL" can be found in the Github.

Addressing the encountered limiter with the professors, the feedback permitted the use of a large optics if the justification for it was logical, which as mentioned before is not practical for other subsystems. Hence, an approach with a telescope with a more complex system was considered. The selected type was a Cassegrain telescope due to their broad use in the space industry to permit long effective focal lengths and having reduced physical dimensions. For this telescope, a MATLAB code was structured to define the optimal dimensions for both the lenses and the array location. The initial considerations were the effective focal length of 2.4 meters and fixing the original diameter value of 35 cm for the primary lens.

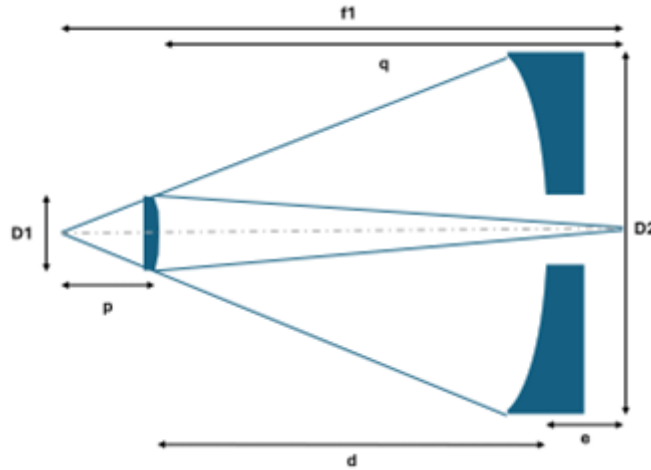


**Figure 4.5 Cassegrain Telescope Layout**

In the graphic representation of the results seen in Figure 4.4, one can observe the tendencies of the secondary diameter ( $D_2$ ), the focal point ( $f_2$ ), and the array location on the length axis ( $e$ ) depending on the distance between the two lenses ( $f_1$ ) which will reflect our physical length.

Based on these tendencies, the objective was to reduce the distance of the array ( $e$ ) in the negative direction as well as maintaining a physical length lower than the original first iteration (1 meter). With these considerations, the selected array distance was 7 centimeters on the negative axis, 10 centimeters in diameter for the secondary mirror, and 75 centimeters for the final physical length of the telescope.

$$m_{\text{telescope}} = \rho_{\text{Al 7075}} \cdot \pi \cdot D_1 \cdot t \cdot 2 - D_2 \cdot 2 \cdot f = 20 \text{ kg} \quad (4.7)$$

$$\rho_{\text{Al 7075}} = 2810 \text{ kg/m}^3 \quad (4.8)$$

$$m_{\text{lenses}} = \rho_{\text{SiC}} \cdot \pi \cdot D_1^2 \cdot t_1 + \rho_{\text{SiC}} \cdot \pi \cdot D_2^2 \cdot t_2 = 6.85 \text{ kg} \quad (4.9)$$

$$m_{\text{total}} = m_{\text{telescope}} + m_{\text{lenses}} + m_{\text{EVK4}} = 29.95 \text{ kg} \quad (4.10)$$

The final part for the optics was the mass and cost estimation for the EVK4 module. The datasheet information already provided a mass of 95 g and a cost of 4000 EUR. For the telescope as a first estimation approach, the density of aluminum 7075 was considered for the volume of a hollow cylinder with the dimensions demonstrated in this section for the physical length and the primary diameter with a thickness of 2 millimeters. In addition, the density of Silicon Carbide was considered for the mass calculations of the primary and secondary lenses, assuming thicknesses of 2 cm and 3 mm respectively. The complete specification data for the optical system is represented in the following table.

## Processor

For processing, it was decided to evaluate NVIDIA's Jetson catalogue since it was the first recommendation for this mission. The original selection was the Jetson AGX Orin in its industrial presentation, although after the discussion with Alesander about the telecommunications requirements, it was decided to select the Jetson AGX Orin in its 32 GB presentation since its capabilities fit the system necessities and both the cost and power are lower than the industrial version, which benefits a redundant design selected for the processor with two units being considered for the design. The last relevant component from the payload is

a solid-state data recorder of 440 GB of storage to safeguard processed data if conditions do not permit an immediate transmission to ground stations. The following table represents the remaining specifications of the components.

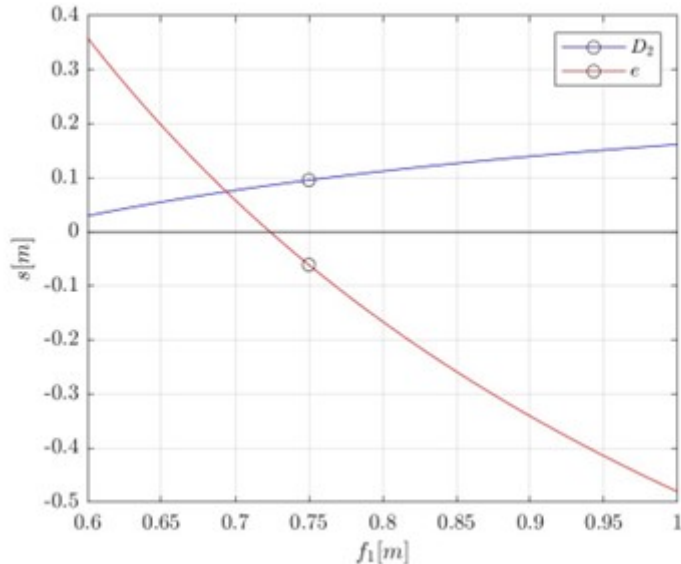


**Figure 4.6** Secondary Lens Diameter and Sensor Distance depending on primary Focal Length

Dimension	Value	Unit	Obtention
Object Distance (h)	31	km	Requirements
Ground Sampling Distance	6	cm	Requirements
Wavelength	700	nm	Max. Visual Range
Pixel Radius	4.86	μm	Specification
Pixel Array	1280 x 720	pixels	Specification
Effective Focal Length	2.43	m	Fixed First Iteration
Focal Length	75	cm	Cassegrain Calculation
Diameter 1	36	cm	Calculation
Diameter 2	11	cm	Calculation
Mass	27	kg	Calculation
Price	10000	EUR	Datasheet

**Table 4.11** Final optical system specifications

Specification	Jetson AGX Orin 32 GB	Mercury RH3440 SSD
Quantity	2	2
Performance	200 TOPS / 930 MHz	440 GB
Power Consumption	15 – 40 W	14 W
Mass	1 kg	1.3 kg
Price	1800 EUR	3000 EUR
Dimensions	100 x 87 mm	160 x 100 mm

**Table 4.12** Processor and data recorder specifications. [7]

### 4.5.2 Attitude Determination and Control System (ADCS) (Keval Ghetiya)

#### Purpose

In this chapter, the preliminary design of the onboard Attitude Determination and Control System (ADCS) is discussed. The purpose of this subsystem is to:

- Determine the spacecraft's attitude.
- Orient the spacecraft according to operational requirements.
- Reject external and internal disturbance torques to maintain a stable configuration.

It is assumed that the launcher will place the spacecraft in a stable configuration within the target orbit.

#### Modelling of the Disturbance Environment

For the sizing and designing of the ADCS, only external disturbance torques are considered due to the limited detailed knowledge of internal components and the simplicity of the design process.

#### External Torques

Using a MATLAB script and formulae from [23], to perform the necessary calculations, the following results were obtained:

- Torque due to Solar Radiation Pressure:

$$T_s = \frac{\phi}{c} A_s (1 + q) (cp_s - cm) \cos \phi = (2.9013 \times 10^{-6}) Nm \quad (4.11)$$

- Torque due to Atmospheric Drag:

$$T_a = \frac{1}{2} \rho C_d A_r V^2 (cp_a - cm) = (2.2500 \times 10^{-7}) Nm \quad (4.12)$$

- Torque due to Magnetic Field:

$$T_m = DB = D \left( \frac{M}{R^3} \lambda \right) = (2.0145 \times 10^{-5}) Nm \quad (4.13)$$

- Torque due to Gravity Gradient:

$$T_g = \frac{3\mu}{2R} |I_z - I_y| \sin(2\theta) = (1.144 \times 10^{-6}) Nm \quad (4.14)$$

The maximum torque, due to the magnetic field, is considered in the selection process of the control method and sizing the actuators.

#### Selection of Control Method

Considering the accuracy and slew requirements, an active control method was chosen. The 3-axis stabilization method was selected due to its successful heritage in many space missions and its ability to control the spacecraft in all three axes. The main trade-off involved balancing performance and scope against cost, with manageable complexity.

## Selection and Sizing of ADCS Hardware: Actuators

Control torques in a 3-axis system come from combinations of two or more actuators for better stability and rotation speed. Options considered included:

- **Control Moment Gyros (CMG):** Suitable for high-torque applications but not ideal in terms of cost, mass, and power budget.
- **Reaction Wheels:** Commonly used for 3-axis stability due to their lower mass, lower power consumption, and accurate momentum exchange capability. Reaction wheels were chosen as the main actuators. An attitude error in the spacecraft results in a control command that torques the wheels, providing a reaction torque that corrects the error.

Sometimes it is necessary to remove the aggregated momentum due to the absorbed torques. This is why secondary actuators are used to dump that momentum. Magnetic Torquers and Thrusters are good possible options for that. Here, cold-gas thrusters are used, considering the ease of integration with the propulsion design.

**Reaction Wheel Calculations:** All the calculations are based on The new SMAD [23].

- Maximum disturbance torque:  $4.029 \times 10^{-5}$  Nm (Torque due to the magnetic field  $\times$  2 margin factor)
- Torque to slew the spacecraft around the Y-axis by 30 degrees in 5 minutes: 0.00116 Nm
- Momentum storage in reaction wheels (assuming max torque accumulates over an orbit): 0.1216 Nms

Four reaction wheels are used, three for each axis and one for redundancy, with a capacity to produce the required torques and store the momentum. The seemingly high margin in sizing the reaction wheels is due to the negligible difference in mass and power consumption of slightly lower capacity wheels.

- Reaction Wheel Torque: 10 mNm
- Reaction Wheel Momentum Storage: 0.5 Nms

Cold-gas thrusters are designed to correct the attitude and dump the momentum created by the reaction wheels. The main driver for their design is the torque required to dump the momentum, not the disturbance or slew torques.

### Thrust Calculations:

- Thrust to reject disturbance torque:  $2.5181 \times 10^{-5}$  N
- Thrust to slew the spacecraft (assuming 5-second acceleration/deceleration): 0.0218 N
- Thrust to dump the momentum with a 1-second burn: 0.1520 N

With some margin, six cold-gas thrusters are set to produce 250 mN of thrust each.

## Selection of ADCS Hardware: Sensors

Several sensor options were considered for attitude determination:

- **Gyroscopes:** Not used due to their complexity.
- **Star Sensors:** Highly accurate but not ideal due to the system's lower accuracy requirements.
- **Sun Sensors:** Six sun sensors are used in multiple directions to measure the spacecraft's attitude.
- **Horizon Sensors:** Two horizon sensors are used during eclipse periods for attitude measurement in LEO, due to their lower mass and power consumption.
- **Magnetometer:** Used as a complementary sensor to provide more accurate results and a different concept for attitude determination.

## Interface with Other Subsystems

The ADCS depends on other subsystems, such as structure. Attitude needs will impose requirements on power and propulsion subsystems, necessitating more power and propellant. The mission needs, particularly the payload/Event Camera pointing requirements, will also influence the ADCS design.

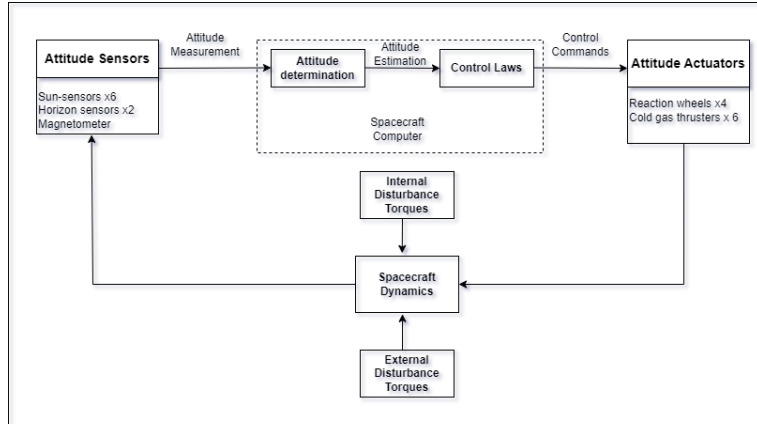


**Figure 4.7** ADSC System [23]

### 4.5.3 Power (Alejandro Oteo, Jessica Hauschulz)

For the design of the power subsystem, the power consumers were first identified, determining their operating periods and power consumption.

Name	Subsystem	Power Consumption (W)	Number components	Period
Jetson origin	Payload1	40	1	Both
SDR	TTC	7	1	Both
S Band Antenna Comercial	TTC	4	1	Both
S-Band Antenna Comercial	TTC	4	1	Both
TTC actuator	TTC	5	2	Both
Event Camera	Payload2	1.5	1	Daylight
Cassegrain Optic	Payload2	45	1	Daylight
SSD	Payload1	14	1	Both
Heater	Thermal	80	1	Eclipse
Sun sensors	ADCS	0	1	Daylight
Horizon sensors	ADCS	4	1	Daylight
Magnetometer	ADCS	0.75	1	Daylight
Reaction Wheels	ADCS	3	3	Daylight
Cold gas thrusters	Propulsion	30	1	Daylight
Propulsion	Propulsion	36	1	Daylight
Solar Arrays	Power	5	1	Daylight
Modular Power System	Power	5	1	Both

**Table 4.13** Power Consumers and Their Operating Periods

The operating periods were either during daylight or during eclipse periods. Subsequently, the "worst-case scenario" was calculated by summing the power consumption of all consumers operating simultaneously (without considering redundancies). This resulted in power requirements of 215W during daylight, 159W during eclipses, and 295.25W for the "worst-case scenario."

After establishing the power requirements, the main components for the system were selected: batteries for the eclipse periods and solar panels, with an aim to minimize weight and maximize initial efficiency.

- **Batteries:** Blue Canyon Tech 28V Batteries 1P8S [18]
- **Solar panels:** Blue Canyon Tech 12U triple panel Array (personalized) [19]

Once the components were identified, the initial parameters were extracted from the datasheets to calculate the system requirements, including battery capacity and the necessary surface area of the solar panels.

$$\text{total power daylight} = \sum(\text{power consumption}(i) \times \text{day components}(i)) \quad (4.15)$$

$$\text{total power eclipse} = \sum(\text{power consumption}(i) \times \text{eclipse components}(i)) \quad (4.16)$$

$$\text{worst case power} = \sum(\text{power consumption}(i) \times \text{number of components}(i)) \quad (4.17)$$

$$\text{final efficiency} = \text{initial efficiency} \times (1 - \text{inherent degradation})^{\text{design lifetime}} \quad (4.18)$$

$$\text{daylight duration} = \text{orbital period} - \text{eclipse duration} \quad (4.19)$$

$$\text{aspr} = \frac{(\text{apd} \times \text{dd}) + (\text{ape} \times \text{ed})}{\text{dd}} \quad (4.20)$$

$$\text{single panel area} = \frac{\text{single panel power}}{\text{sun flux} \times \text{initial efficiency} \times \text{efficiency system}} \quad (4.21)$$

$$\text{required solar array area} = \frac{\text{average solar power required}}{\text{sun flux} \times \text{final efficiency} \times \text{efficiency system}} \quad (4.22)$$

$$\text{estimated mass of solar array} = \text{required solar array area} \times \text{mass per area} \quad (4.23)$$

$$\text{num panels required} = \left\lceil \frac{\text{required solar array area}}{\text{single panel area}} \right\rceil \quad (4.24)$$

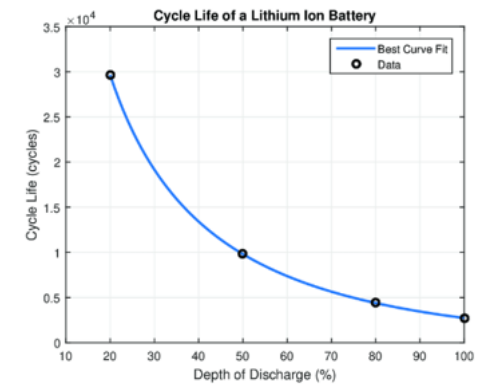
$$\text{total power solar panels} = \text{num panels required} \times \text{single panel power} \quad (4.25)$$

$$\text{cycles} = \frac{\text{design lifetime} \times (365 \times 24 \times 3600)}{\text{orbital period}} \quad (4.26)$$

$$\text{battery dod} = \frac{\text{DoD corresponding to cycles from CycleLife}}{100} \quad (4.27)$$

For calculating the Depth of Discharge (DoD), a linear interpolation is performed using the provided cycle life data (*CycleLife*) and the corresponding Depth of Discharge data (*DoD*). The interpolation estimates the DoD value at a specific number of cycles (*cycles*). This process ensures that the DoD value accurately reflects the battery's performance over its expected cycle life. The interpolated DoD value is then divided by 100 to convert it to a percentage.

$$\text{energy required during eclipse} = \text{average power eclipse} \times \text{eclipse duration} \quad (4.28)$$

**Figure 4.8** DoD for a Lithium Ion Battery

$$\text{total battery storage capacity required} = \frac{\text{energy required during eclipse}}{\text{battery dod}} \quad (4.29)$$

$$\text{battery capacity required} = \frac{\text{total battery storage capacity required}}{\text{nominal battery voltage}} \quad (4.30)$$

$$\text{num battery packs} = \left\lceil \frac{\text{total battery storage capacity required}}{\text{battery capacity}} \right\rceil \quad (4.31)$$

$$\text{total battery mass} = \text{num battery packs} \times \text{battery mass} \quad (4.32)$$

**aspr** average solar power required

**apd** average power daylight

**dd** daylight duration

**ape** average power eclipse

**ed** eclipse duration

Using these formulas, a MATLAB program was developed to calculate the system, yielding the following values:

#### 4.5.4 TT&C (Alesander Oteo)

The first approach set the data that is transmitted by the spacecraft to the ground according to the mission objectives. As a result, the spacecraft sends the orbit and the size of the detected objects, all determined by the payload.

Once the main content of the message was determined, it was decided that the orbit of the debris would be indicated using the TLE format. [20]

#### TLE Format

A two-line element set (TLE) is a data format that encodes the orbital elements of an Earth-orbiting object at a specific moment in time, known as the epoch. A proper explanation of how the TLE format works can be found in [8]. This format was introduced by NORAD . The TLE format encodes the orbital elements of an Earth-orbiting object into two 69-column ASCII lines, preceded by a title line.

Parameter	Value
Initial efficiency	30.00%
Final efficiency	29.26%
Total power required during daylight (W)	205.25
Total power required during eclipse (W)	159.00
Worst Case Power Consumption (W)	295.25
Energy required during eclipse (Wh)	53.36
Number of Cycles	26056.83
Depth of Discharge (percentage)	0.26
Total battery storage capacity required (Wh)	205.91
Battery capacity required (Ah)	7.35
Number of battery packs required	3
Total battery mass (kg)	1.95
Required solar array area (m <sup>2</sup> )	0.88
Single panel Area (m <sup>2</sup> )	1.24
Number of commercial solar panels required	1
Total solar panel provided power (W)	354.00

**Table 4.14** Power Subsystem Results

**Figure 4.9** TLE format structure [1]

## **Structure of the Message**

Once it was clear what to send to the earth and how, the content and structure of the message were fixed:

Component	Size
Start	1 Byte
Identifier	1 Byte
Size	2 Bytes
Line 1 of TLE	69 Bytes
Line 2 of TLE	69 Bytes
End	1 Byte

**Table 4.15** Structure of the Message

## Components of the Data Frame

- **Start Delimiter (1 byte):** Marks the beginning of a new data frame. A specific character or agreed byte easily identifiable by the receiver.

- **Object Size (2 bytes):** Size of the detected object in cm, with 8 bits for the integer part and 8 bits for the fractional part, allowing precision to 1/256 cm.
- **Identifier Number (1 byte):** Unique number for each object, representing up to 256 unique identifiers (0-255).
- **Line 1 of TLE (69 bytes):** First line of the Two-Line Element set, encoding various orbital parameters [20].
- **Line 2 of TLE (69 bytes):** Second line of the TLE, providing additional orbital parameters [20].
- **End Delimiter (1 byte):** Marks the end of a data frame, ensuring complete frame reception and parity check [24]

This creates a data frame of 143 bytes. A limitation to the transmission of 30 objects is set, making the whole message 4290 bytes long.

## Carrier Band

The S-band was selected for the mission following the information gathered in [10]. According to it, “Satellite Tracking, Telemetry & Command (TT&C) is typically conducted over S-band”.

The S band is a designation by the IEEE for a part of the microwave band of the electromagnetic spectrum covering frequencies from 2 to 4 gigahertz (GHz). The S band is widely used by different applications as airport surveillance radar, weather radar, surface ship radar, and satellites, even WIFI (the IEEE 802.11b and 802.11g) uses it. One of the main advantages of it is that higher frequency bands of transmitters require higher power inputs, so here this band has an advantage.

## System Architecture

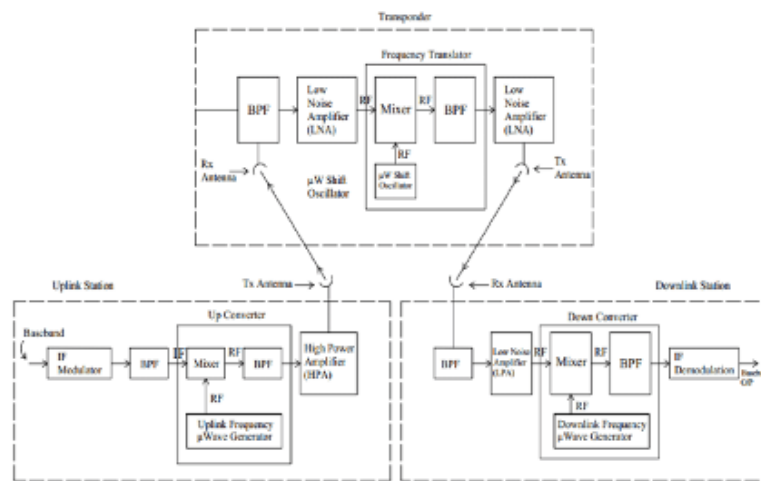


**Figure 4.10** Typical TT&C structure

These are the typical components of a communication system [10]: Radio or Modulator/Demodulator, Mixers, Filters, Amplifiers, Antenna, Encryption, Spread-Spectrum Communication

Having this in account, the subsystem was defined. Components were selected to find the best fit. Two S-band Antennas and an SDR were chosen, as they integrate all listed components, and are designed to work together, making them the best match. To connect them, a coaxial cable of maximum 60 cm was selected, looking for the minimum loss, as both the antennas and the SDR have a SMA connector. [5]

These components are:

- **S-Band Antenna:** S-Band Antenna Commercial from Endurosat.
- **SDR:** Versatile Wideband SDR from Endurosat.
- **Coaxial cable:** LMR-400

With an attenuation due to the connexion cable of  $0.187 \text{ dB/m}$ , for  $60\text{cm}$  we have a loss of  $0.1122 \text{ dB}$  [17]. Knowing this, here are the characteristic values of the TT&C subsystem:

Parameter	Value
Antenna Power	36.02 dBm
Cable Attenuation	0.1122 dB
Antenna Gain	7 dB
Distance	799 km
Frequency	$2.1 \times 10^9 \text{ Hz}$
Receiving Antenna Gain	40 dB
EIRP	42.91 dBm
Free Space Path Loss (FSPL)	118.33 dB

**Table 4.16** Values used and results of the TTC subsystem

For sizing the EIRP and the Free Path Loss, these formulas are used:

$$\text{EIRP}_{\text{dBm}} = P_{\text{trans\_dBm}} - \text{Cable\_atten\_dB} + G_{\text{ant\_dB}} \quad (4.33)$$

$$\text{FSPL}_{\text{dB}} = 20 \log_{10}(d_m) + 20 \log_{10}(f_{\text{Hz}}) + 20 \log_{10}\left(\frac{4\pi}{c}\right) - G_{\text{tx\_dB}} - G_{\text{rx\_dB}} \quad (4.34)$$

#### 4.5.5 Ground Segment (Alesander Oteo)

Ground stations were selected based on SMAD recommendations for LEO, high inclination, and low eccentricity orbits: “Ground stations at high latitude locations provide coverage for almost every orbit each day.” [23]

Most stations are above  $50^\circ$  latitude to ensure optimal global coverage. They transmit commands at 2030 MHz to avoid interference with the downlink, as the satellite is using the same antennas for both up- and down-link. Their strategic placement supports most satellite ground tracks.

City	Latitude	Longitude	City	Latitude	Longitude
Reykjavik, Iceland	64.1355	-21.8954	Yekaterinburg, Russia	56.8389	60.6057
Belfast, United Kingdom	54.5973	-5.9301	Novosibirsk, Russia	55.0084	82.9357
Bergen, Norway	60.3913	5.3221	Sapporo, Japan	43.0618	141.3545
Copenhagen, Denmark	55.6761	12.5683	Anchorage, USA	61.2181	-149.9003
Stockholm, Sweden	59.3293	18.0686	Vancouver, Canada	49.2827	-123.1207
Helsinki, Finland	60.1695	24.9354	Seattle, USA	47.6062	-122.3321
Saint Petersburg, Russia	59.9343	30.3351	Calgary, Canada	51.0447	-114.0719
Moscow, Russia	55.7558	37.6173	Edmonton, Canada	53.5461	-113.4938

**Table 4.17** Selected Ground Stations

#### 4.5.6 Structure (Roberto Aguiñaga and Kiyan Boetzel)

Initial mass estimates and the final total and component masses are shown in Tab.4.18.

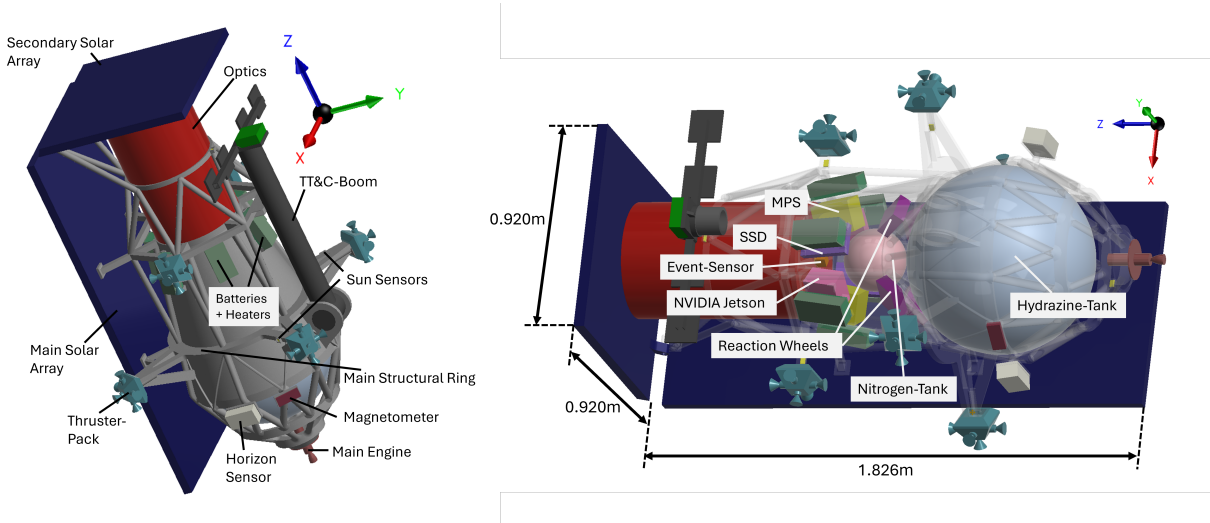
### Structure and Configuration

In the stowed configuration, the spacecraft has length of 1.826 m, with a width and height of 0.920 m. the component arrangement is shown in Fig.4.11, with the deployed vehicle configuration shown in Fig.4.12. The x-axis is defined along the inverse vehicle velocity vector, while the z-vector points in the direction of observation.

The main drivers for the structural design were the propulsion system tanks and the the main payload optics. To minimize the effects of a changing centre of mass, the tanks and optics were arranged in-line, connected by a conical structural bus, ending in the main strutural ring. A truss structure secures the main engine. The pyramidal reaction wheel arrangement is located on the nitrogen tank structural connectors, over the vehicle centre of mass. The computation and power management components are stored inside the main bus, while six heater-covered batteries are mounted on the outside. Around the main conical bus, a secondary truss structure provides the support and additional stiffness for the optics and solar arrays. The dual panels yield a total solar array area of  $1.537 \text{ m}^2$ . Not shown here is a layer of Multi-Layer-Insulation (MLI) around the vehicle.

As the spacecraft only rotates between  $\pm 15^\circ$  wrt. the orbital plane normal vector, a fixed mount for the TT&C subsystem was not possible. to maintain uninterrupted communication and data transmission to ground stations, the TT&C system is mounted on a separate boom which deploys from the vehicle and enables antenna direction in two axes. This arrangement significantly decreases the requirement on the AOCS system by limiting the spacecraft rotation. The TT&C boom uses either carbon composites or kevlar to save mass.

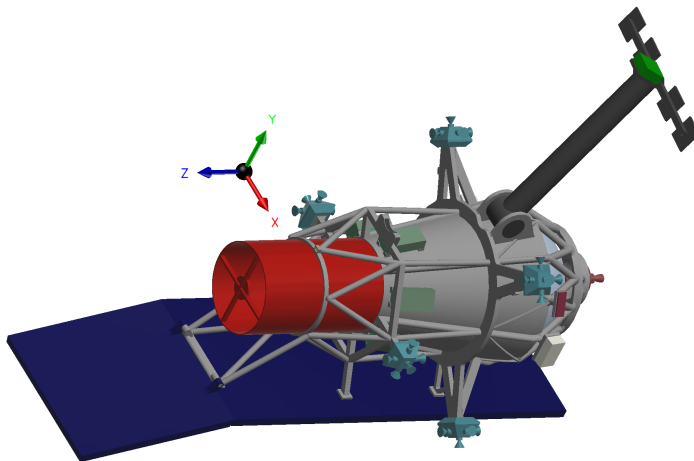
Four AOCS thrusters are mounted on beams coming off the main structural ring. an additional pair is mounted further forward, serving as redundant units.



**Figure 4.11** Vehicle Dimensions, Structure, and Modules (Stowed)

### Launch Vehicle Interface

The final vehicle volume exceeds the largest available side-mounted payload spot on the rideshare stack, therefore only the so-called “cake-topper” on top of the rideshare-stack remains as an option. This limits

**Figure 4.12** Final deployed Configuration

<b>Component</b>	<b>Mass [kg]</b>	<b>Mass Fraction [%]</b>	<b>Initial Estimation [%]</b>
Payload	27.92	11.99	20 – 30
Power	14.01	6.02	20 – 25
TT&C	9.75	4.19	10 – 20
Thermal	0.02	0.009	5 – 10
Propulsion	87.04	34.39	5 – 10
AOCS	34.08	14.64	10 – 15
Structure	60.01	25.78	15 – 20
<b>Total (Beginning of Life) <math>m_{B.o.L.}</math></b>	<b>232.79</b>	-	-
<b>Total (Dry) <math>m_{Dry}</math></b>	<b>187.32</b>	-	-

**Table 4.18** Component Mass distribution

the launcher- flexibility and increases the launch costs, therefore it is a non-ideal solution.

The payload on a "cake-topper" mount must be able to withstand axial accelerations of between 5.0 g to 9.5 g, which is however lower than the loads expected for a similarly sized payload on a lateral mount  $\pm 11.0\text{ g}$ . Lateral accelerations of  $\pm 5.0\text{ g}$  are expected, which are similar to those expected for a lateral mounting[15, 14]. While the acceleration limits for the cake-topper are (in this case) lower than for a lateral mount, the length of the vehicle leads to a high moments of inertia  $I_{xx} = 49.276 \text{ kg m}^2$  and  $I_{yy} = 50.139 \text{ kg m}^2$  with respect to the centre of gravity. These high moments of inertia can lead to excessive vibrations and high lateral moments, if not mitigated.

To reduce these effects, a mounting point close to the centre of gravity on the main structural ring 4.11, via an additional adapter-truss, was chosen. While this increased the weight and therefore launch costs slightly, it reduced the need for strengthening against lateral moments.

#### 4.5.7 Thermal (Roberto Aguiñaga, Jessica Hauschulz)

The first approach was replicated from the steps carried out during the practical course for this system where an excel sheet was set up with the formulas required to calculate the hot case and a cold case. At this point of the iteration process, there were no fixed dimensions for the spacecraft; hence a case of study was considered based on the common dimensions of a LEO earth observation satellite with a mass of about 500 kg, which was the maximum for this project. The dimensions were based on the South Korea spacecraft CAS 500 having a squared base of 1.9 x 1.9 meters and a length of 2.9 meters.

For this first approach, fixed values for the sun flux and the earth energy flux were established at  $1370 \text{ W/m}^2$  and  $237 \text{ W/m}^2$ , respectively. The absorptance and emissivity values were first considered as if the

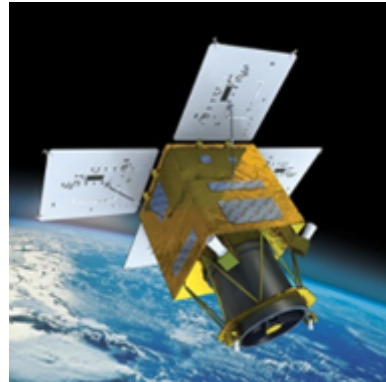


**Figure 4.13** Reference Satellite CAS 500 from Korean Aerospace Research Institute [6]

satellite was coated with white paint, therefore using 0.2 and 0.9 as the respective factors. A value of 0.42 was considered for albedo and a view factor of 0.79 for the view factor with respect to the mission's altitude. The area considered for the solar heat was one of the larger sides of the satellite ( $1.9 \times 2.9 \text{ m}^2$ ) while the infrared and albedo cases considered the squared base ( $1.9 \times 1.9 \text{ m}^2$ ). The considered power consumption by the satellite was estimated to be approximately 200 W with a dissipation factor of 0.7.

$$Q_{\text{TOTAL HOT}} = Q_{\text{SUN}} + Q_{\text{ALBEDO}} + Q_{\text{IR}} + Q_{\text{INT}} = 3852 \text{ W} \quad (4.35)$$

$$Q_{\text{SUN}} = \alpha \phi_{\text{SUN}} A_{\text{SUN}} = 1563 \text{ W} \quad (4.36)$$

$$Q_{\text{ALBEDO}} = Q_{\text{SUN}} \cdot F = 750 \text{ W} \quad (4.37)$$

$$Q_{\text{IR}} = \alpha \phi_{\text{earth}} A_{\text{earth}} = 1439 \text{ W} \quad (4.38)$$

$$Q_{\text{INT}} = 200 \text{ W} \cdot 0.5 = 100 \text{ W} \quad (4.39)$$

$$Q_{\text{TOTAL COLD}} = Q_{\text{ALBEDO}} + Q_{\text{IR}} + Q_{\text{INT}} = 2289 \text{ W} \quad (4.40)$$

$$T = \left( \frac{Q_{\text{TOTAL}}}{\epsilon \sigma A_{\text{TOTAL}}} \right)^{1/4} \quad (4.41)$$

$$T_{\text{HOT}} = -47^\circ\text{C} \quad (4.42)$$

$$T_{\text{COLD}} = -74^\circ\text{C} \quad (4.43)$$

The first calculation resulted in both hot and cold cases giving negative values below 40 degrees Celsius, which was non-conforming for the desired minimum value of 10 degrees and 40 degrees defined by the batteries' capacities. Simultaneously, a second MATLAB calculation was done with different albedo and sun flux values for the hot and cold cases obtained from the SMAD book, although the main difference to the first assumption was the areas here all the surfaces of the satellite except for the one where the optics were located were considered for heat absorption from all surfaces giving an opposite result as before where both hot and cold cases were over 30 degrees. [23]

After meetings within the team, new solar array requirements and structural designs reduced the satellite's dimensions, and the surfaces that were absorbing radiation were limited by the solar panels oriented

to the sun during the entire orbit. For the next iterations, the influence of the sun radiation was neglected for both hot and cold cases, and having a cylindrical shape, half of the cylindrical surface was radiated by the albedo and infrared heat. The area considered from this point was  $1.47 \text{ m}^2$  out of the total surface area of  $3.72 \text{ m}^2$ . With these new considerations, the results from the code for a satellite with no insulation in the hot case was 14 degrees and minus 11 for the cold case, values that were closer to the desired temperature range, nonetheless would not permit the batteries to operate in the cold case.

The code was set to evaluate several multilayer insulations specifications as well. With the original spacecraft sizing assumptions, the Double Aluminized Mylar of 2 millimeters served as an optimal option for insulation. After structural modifications, this was unfortunately not the case, which led the team to research for more MLI solutions available. For the final iteration, a combination of 1 layer of Chemglass 250 covered with a 0.5-millimeter Silvered Teflon coating permitted an absorptance of 0.05 combined with an emissivity of 0.78. The calculations with the new insulation properties increased the temperature for both cases, getting a hot case of 20 degrees for the hot case, which was already compliant with the subsystem's thermal requirements. The cold case still demonstrated a below zero value of -5 degrees, which led the team to size an active thermal solution. After researching for available options for space applications, electric Kapton foil heaters were selected for their efficiency in power consumption and low values for mass and dimensions, which now permitted the cold case to remain above zero degrees Celsius. The calculated heater power consumption was below 10 W and the selected heater can get up to 40 W, combined with a thermal sensor, the desired temperature can be ensured for the batteries during cold phases of the mission.

## 4.6 Conclusion (Roberto Aguiñaga)

To finalize the report, it would be relevant to highlight the main sources for changes, which made the time run through several iterations during the semester. While the first driver was the payload, once a telescope approach was defined, the sizing for the subsystem was not deviating anymore. What the team would consider as the main source of deviation, was the definition of an optimal orbit, to enable the accuracy required for recording at conjunctions and data transfer to ground, the orbit subsystem was run through multiple simulation iterations in GMAT. In some occasions, this led to the readjustment of the rest of the subsystems, mainly for power and subsequently thermal subsystems. Communication within members remains as a critical factor for the success of an optimal spacecraft subsystem sizing, in an environment where each component can have a high level of interdependence with others, it is required to define a centralized workbench and structure. Communication and organization within the members is another relevant, if not the main factor involved in the success of the mission on time and with quality. Communication in combination with a strong and centralized structure ever since the definition of requirements would improve the efficiency and reduce the iterations required for objective completion.

## Bibliography

- [1] ADCOM. Adcom do form 12, December 1978.
- [2] F. Isler V Bisulco, A. Cladera and D. Lee. Near-chip dynamic vision filtering for low-bandwidth pedestrian detection. Technical Report IEEE Computer Society Annual Symposium on VLSI, Samsung Research, Samsung Artificial Intelligence Center New York, 2020.
- [3] Sony Semiconductor Solutions Corporation. Event-based vision sensor (evs). <https://www.sony-semicon.com/en/products/is/industry/evs.html>, 2023.
- [4] Sony Semiconductor Solutions Corporation. Event filter function for streamlined information acquisition. <https://www.sony-semicon.com/en/news/2021/2021090901.html>, 2024.
- [5] EnduroSat. S-band antenna commercial datasheet, 2024.
- [6] KARI. Cas500 (compact advanced satellite 500). <https://www.eoportal.org/satellite-missions/cas500#missionstatus>, 2022.
- [7] Karubunathan, Leela. *NVIDIA Jetson AGX Orin Series, Technical Brief*. NVIDIA Corporation], |2788 San Tomas Expressway, Santa Clara, CA, 2022.
- [8] Nick Kuhl, Kai Perlmutter, and Bryan Welch. Strategic center for networking, integration, and communications orbit propagation front-end software development. Technical Report NASA/TM-2018-219992, NASA Glenn Research Center, Cleveland, Ohio, November 2018.
- [9] Chiara Manflettis. Rocket propulsion. Lecture notes, 2024. Lecture notes for the subject Rocket Propulsion.
- [10] NASA. Small spacecraft technology state of the art: Communications. <https://www.nasa.gov/smallsat-institute/sst-soa/soa-communications/#9.2.1>, 2024.
- [11] Prophesee. *EVK4 Camera Manual 1.1*. PROPHESEE S.A., 75012, Paris, France, 2023.
- [12] Aerojet Rocketdyne. In-space propulsion data sheets, 2020.
- [13] H. Ryu. Industrial dvs design; key features and applications. Technical report, Samsung Electronics, 2020.
- [14] Space Exploration Technologies Corp. (SpaceX), Hawthorne, CA. *Cake Topper Payload User's Guide*, January 2023. Available at [https://storage.googleapis.com/rideshare-static/Cake\\_Topper\\_Payload\\_Users\\_Guide.pdf](https://storage.googleapis.com/rideshare-static/Cake_Topper_Payload_Users_Guide.pdf).
- [15] Space Exploration Technologies Corp. (SpaceX), Hawthorne, CA. *Rideshare Payload User's Guide*, 9th edition, December 2023. Available at [https://storage.googleapis.com/rideshare-static/Rideshare\\_Payload\\_Users\\_Guide.pdf](https://storage.googleapis.com/rideshare-static/Rideshare_Payload_Users_Guide.pdf).
- [16] SpaceX. *Falcon 9 users guide*, September 2021. Available at [https://storage.googleapis.com/rideshare-static/Cake\\_Topper\\_Payload\\_Users\\_Guide.pdf](https://storage.googleapis.com/rideshare-static/Cake_Topper_Payload_Users_Guide.pdf).
- [17] Times Microwave Systems. Lmr-400-75 datasheet, 2024.
- [18] Blue Canyon Technologies. Batteries datasheet, 2024.

- [19] Blue Canyon Technologies. Power systems datasheet, 2024.
- [20] David A. Vallado and Paul Crawford. Sgp4 orbit determination. In *AIAA/AAS Astrodynamics Specialist Conference and Exhibit*, Honolulu, Hawaii, August 2008. American Institute of Aeronautics and Astronautics.
- [21] Ulrich Walter. *Astronautics*. Springer Cham, Cham, 3rd edition, 2018.
- [22] Kevin Weeden, Brian Shortt. Development of an architecture of sun-synchronous orbital slots to minimize conjunctions. *Proceedings of the National Academy of Sciences*, 2008.
- [23] D. Puschell Jeffrey Wertz, J. Everett. *Space Mission Engineering: The New SMAD*. Microcosm Press, Hawthorne, CA, 2011.
- [24] Rodger E. Ziemer and William H. Tranter. *Principles of Communications: Systems, Modulation, and Noise*. Wiley, New York, 7th edition, 2024.